Carbohydrate Polymers 83 (2011) 1828–1833

Contents lists available at ScienceDirect

Carbohydrate Polymers

journal homepage: www.elsevier.com/locate/carbpol

Preparation and properties of thermoreversible hydrogels based on methoxy poly(ethylene glycol)-grafted chitosan nanoparticles for drug delivery systems

Yanqin Liang [a], Liandong Deng [a], Chen Chen [a], Juan Zhang [a], Ruimei Zhou [a], Xu Li [b], Renjie Hu [b], Anjie Dong [a,*]

[a] School of Chemical Engineering and Technology, Tianjin University, Tianjin 300072, China
[b] Tianjin Institute of Medical and Pharmaceutical Science, Tianjin 300020, China

ARTICLE INFO

Article history:
Received 14 September 2010
Received in revised form 20 October 2010
Accepted 20 October 2010
Available online 28 October 2010

Keywords:
Methoxy poly(ethylene glycol)-grafted chitosan
Thermoreversible hydrogel
Nanoparticles
Drug delivery
Cytotoxicity

ABSTRACT

A thermoreversible nanoparticle hydrogels based on carboxylated methoxy poly(ethylene glycol)-grafted chitosan (*N*-CS-g-mPEG) were investigated in this paper. The aqueous dispersion of *N*-CS-g-mPEG nanoparticle freeze-dried powder (NP-FDP) can undergo reversible gel–sol transition as the temperature changes. The structures of *N*-CS-g-mPEG NPs and hydrogels were characterized by TEM, DLS and ESEM. Using 5-Fluorouracil (5-FU), bovine serum albumin (BSA) and dexamethasone (DXM) as model drugs, *in vitro* release behaviors of drug-loaded hydrogels were also investigated. The release results show that there is a sustained release of BSA and DXM from the drug-loaded hydrogel. *In vitro* cytotoxicity tests investigated by MTT assay indicate that *N*-CS-g-mPEG is non-toxic to normal mouse embryonic fibroblast cells (3T3). Therefore, the thermoreversible *N*-CS-g-mPEG NP hydrogels could be potentially applied in a local minimally invasive drug delivery system.

1. Introduction

The thermoreversible gelation of biodegradable polymer aqueous solutions, i.e. reversible sol–gel transition with the changes of temperature, have been extensively studied during the past decade. Typically, they are an aqueous solution at room temperature (20 °C) or lower and form a semisolid gel at the body temperature (37 °C), and the gel can become a free-flowing liquid again as the temperature decreases (Joo, Park, Choi, & Jeong, 2009). Therefore, the thermoreversible gels are of great interest in drug delivery systems, cell encapsulation, tissue engineering (Hatefi & Amsden, 2002; Shu, Liu, Palumbo, Luo, & Prestwich, 2004; Temenoff & Mikos, 2000), and biomedical devices (Jeong, Kim, & Bae, 2002; Kumar, Muzzarelli, Muzzarelli, Sashiwa, & Domb, 2004).

In particular, the thermosensitive hydrogels have been extensively studied for drug delivery (Qiu & Park, 2001). These systems are injectable fluids that can transform into gels in situ at body temperature (Hoffnam, 2002). Injectable hydrogels do not require a surgical procedure for implantation, and various therapeutic drugs can be incorporated through simple mixing (Bhattarai, Matsen, & Zhang, 2005; Park et al., 2009). As commercially available thermogelling polymers, copolymers of poly(ethylene oxide) and poly(propylene oxide) (known as poloxamer) (DesNoyer & McHugh, 2003; Exner, Krupka, Scherrer, & Teets, 2005; Roques, Salmon, Fiszman, Fattal, & Fromes, 2007) and copolymers of *N*-isopropylacrylamide (Coughlan, Quilty, & Corrigan, 2004; Maeda & Yamabe, 2009; Zhang, Bhat, & Jandt, 2009) have been widely investigated for biomedical applications. However, the application of these systems is limited because they are not biodegradable. Therefore, the biodegradable hydrogels have been designed using natural polymers that are susceptible to enzymatic degradation (Muzzarelli, 1997). Chitosan have received a great deal of attention due to their well documented biocompatibility, bioactivity and low toxicity (Lehr, Bouwstra, Schacht, & Junginger, 1992; Mi, Shyu, Chen, & Schoung, 1999; Roughley et al., 2006). These and other intrinsic properties (e.g. hydrophilicity, functional amino groups, and a net cationic charge) have made chitosan an ideal candidate for the intelligent delivery of macromolecular compounds, such as drugs, proteins, and genes (Bhattarai, Gunn, & Zhang, 2010; van der Merwe, Verhoef, Verheijden, Kotzé, & Junginger, 2004). Chitosan can be engineered into different shapes and geometries such as nanoparticles, microspheres, membranes, sponges, rods and hydrogel (Denkbas & Ottenbrite, 2006).

To date, a variety of chitosan-based thermosensitive hydrogels have been studied. Chenite et al. developed a thermosensitive hydrogel based on CS/polyol salt combinations that could undergo sol–gel transition at a temperature close to 37 °C (Chenite et al., 2000). The hydrogels using chitosan co-polymers in combination

* Corresponding author. Tel.: +86 22 27890707; fax: +86 22 27890710.
E-mail address: ajdong@tju.edu.cn (A. Dong).

0144-8617/$ – see front matter © 2010 Elsevier Ltd. All rights reserved.
doi:10.1016/j.carbpol.2010.10.048

with poly(*N*-isopropyl acrylamide) (PNi-PAM) and poloxamer have been recognized as good candidates for in situ, reversible hydrogel formation. An injectable chitosan-based hydrogel from water-soluble chitosan derivatives, chitosan-*graft*-glycolic acid (GA) and phloretic acid (PA) (CH-GA/PA), has been developed by Jin et al (Jin et al., 2009). Bhattarai et al. described PEG-grafted chitosan as an injectable thermosensitive hydrogel for sustained drug release and tissue engineering (Bhattarai, Ramay, Gunn, Matsen, & Zhang, 2005). In this article, we describe the preparation and characterization of carboxylated mPEG-grafted chitosan (*N*-CS-g-mPEG) nanoparticle hydrogel, i.e. the aqueous dispersion of *N*-CS-g-mPEG nanoparticle freeze-dried powder (NP-FDP) can undergo reversible gel–sol transition as the temperature changes. In addition, the gel–sol transition behavior, interior morphology, drug-release behavior and *in vitro* cytotoxicity for these NP hydrogels were also investigated.

2. Experimental

2.1. Materials

Chitosan ($M_n = 5.0 \times 10^4$, degree of deacetylation = 95%) was purchased from Aokang Bio-Technology Co., Ltd. (Shandong, China). Methoxy poly(ethylene glycol) (mPEG) ($M_n = 2000$) was purchased from Aldrich Chemical Co., Inc. (America). 4-Dimethylaminopyridine (DMAP) and 1-ethyl-3-(3-dimethyllaminopropyl) carbodiimide hydrochloride (EDC·HCl) were purchased from Jingchun Reagent Co., Ltd. (Shanghai, China). N-hydroxysuccinimide (NHS) was purchased from J&K Chemical Co., Ltd. (Beijing, China). 5-Fluorouracil (5-FU) was purchased from Bangcheng Chemical Co., Ltd. (Shanghai, China). Bovine serum albumin (BSA, $M_n = 66$ kDa) was supplied by Roche Company. Dexamethasone (DXM) was provided by Yilong Co. (Guangzhou, China). Coomassie brilliant blue G250 was purchased from Biosharp Company. Succinic anhydride, 1,4-dioxane, diethyl ether (anhydrous) and ethanol (anhydrous) were obtained from Jiangtian Chemical Technology Co., Ltd. (Tianjin, China). All the reagents were of analytic grade.

2.2. Preparation of N-CS-g-mPEG

N-CS-g-mPEG was synthesized according to the reference Jeong, Kim, Jang, and Nah (2008), and the synthesis details were improved. *N*-CS-g-mPEG was obtained with a two-step technique (Supporting Scheme S1). Briefly, mPEG (1 mmol), succinic anhydride (2 mmol) and DMAP (2 mmol) were dissolved in 1,4-dioxane (100 mL) and stirred under nitrogen protection at 30 °C for 24 h. The filtered solution was precipitated by ice-cold diethyl ether. The precipitate was then filtered, washed with an excess of anhydrous ethanol, and dried under vacuum for 3 days at room temperature to obtain carboxylated mPEG (Jeon, Lee, Kim, Lee, & Kim, 2003). The yield of carboxylated mPEG was about 73%. After carboxylated mPEG (1 mmol) was dissolved in deionized water, the carboxyl of mPEG was activated by EDC·HCl (1.2 mmol) and NHS (1.2 mmol) at pH 4.0–5.0, and stirred at 30 °C for 30 min to obtain a stable amino-reactive intermediates. After chitosan (5 mmol) was well dissolved in the reaction solution at pH 4.0–5.0, the pH value was adjusted to 8.0–9.0, and then the reaction was carried out at 30 °C for 24 h. Subsequently, the reaction solution was adjusted to 4.0–5.0, and dialyzed for 48 h against distilled water using a dialysis tube (Spectrapore, MWCO 8000–12,000) to remove catalyst, and then lyophilized to obtain *N*-CS-g-mPEG-20 white powder. The yield of *N*-CS-g-mPEG-20 was about 80%. *N*-CS-g-mPEG-15 and *N*-CS-g-mPEG-25 were also synthesized by the above method, and *N*-CS-g-mPEG was characterized by FTIR, ^{1}H NMR (Supporting Figs. S1 and S2). The degree of substitution (DS, molar ratio of carboxylated mPEG to monosaccharide residue of chitosan) was determined using a fully automatic ATN-33 nitrogen analyzer (CAM1033455, China) (Table 1).

Table 1
N-CS-g-mPEG synthesized in this paper.

N-CS-g-mPEG-*n*[a]	*N*-CS-g-mPEG-15	*N*-CS-g-mPEG-20	*N*-CS-g-mPEG-25
DS[b]	14.38 ± 0.09%	18.23 ± 0.07%	22.75 ± 0.11%

[a] *n* in *N*-CS-g-mPEG-*n* mean DS calculated theoretically.
[b] DS was determined using a fully automatic ATN-33 nitrogen analyzer.

2.3. Preparation and characterization of N-CS-g-mPEG NPs

The *N*-CS-g-mPEG NPs were prepared by direct dispersion method. Briefly, 10 mg *N*-CS-g-mPEG was dissolved in 2 mL phosphate buffer saline (PBS, pH 7.4) under magnetic stirring, and then the solution was vigorously stirred for 30 min at room temperature. The resulting dispersion was lyophilized to obtain *N*-CS-g-mPEG NP-FDP by employing a freeze dryer system (LGJ-10, Four-Ring, China) (Lin et al., 2008; Zhai et al., 2008).

The sizes and size distribution of *N*-CS-g-mPEG NPs were measured by BI-200SM dynamic laser light scattering (DLS, Brookhaven Instruments Corporation) at 25 °C and at a scattering angle of 90°.

The TEM specimens for *N*-CS-g-mPEG NPs in aqueous dispersions were observed under a JEM-100CX II instrument. Samples were prepared by placing a drop of NP-FDP aqueous dispersion on the Formvar-coated copper TEM grid, and then dyed by phosphatotungstic acid.

2.4. Phase diagram measurement

The thermoreversible gel–sol transition of the *N*-CS-g-mPEG NP aqueous dispersion was determined by the test tube inverting method (Gong et al., 2007; Park et al., 2007; Shim et al., 2006; Sombatmankhong, Sanchavanakit, Pavasant, & Supaphol, 2007; Wu, Su, & Ma, 2006). A 4 mL vial (inner diameter 1.1 cm) containing 0.5 mL of the *N*-CS-g-mPEG NP-FDP aqueous dispersion was incubated at 4 °C for 12 h, which would form no-flow NP hydrogel. The transition temperature was determined by no flow (gel)–flow (sol) criterion when the vial was inverted with a temperature increment of 2 °C per step. Three replicates were performed in each point of with an accuracy of ±0.1 °C.

2.5. Interior morphology of thermoreversible hydrogel

To observe the interior morphologies of *N*-CS-g-mPEG NP hydrogels, the hydrogel samples were quickly frozen in liquid nitrogen and further lyophilized by a freeze dryer system under vacuum at ∼50 °C for at least 48 h until all the water was sublimed. The freeze-dried hydrogels were then fractured carefully and sputter-coated with gold. The interior morphologies of hydrogels were visualized with environmental scanning electron microscopy (ESEM, PHILIPS XL30).

2.6. In vitro drug release

N-CS-g-mPEG NP-FDP was added to phosphate buffer saline (PBS, pH 7.4) containing 5-FU, BSA or DXM (1 wt%), the dispersion (2–3 wt%, 1 mL) was placed in a test tube, and incubated at 4 °C for 12 h to form a hydrogel. After 10.0 mL of phosphate buffer saline (PBS, pH 7.4) was added into the test tube, the tube was set on a constant temperature shaker (SHZ-88, Jiangsu, China) at 37 °C and 70 r/min. At the presetting time, a 5-mL aliquot of PBS was withdrawn for measuring the amount of drug released from the

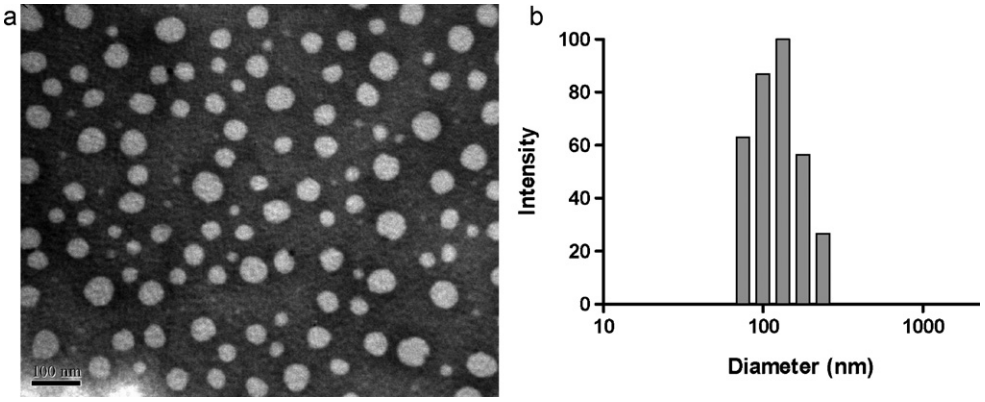

Fig. 1. TEM micrograph (a) and particle size distribution profile (b) of *N*-CS-g-mPEG-20 NPs.

N-CS-g-mPEG NP hydrogel and then an equal volume of fresh PBS was supplemented to keep the volume of the release medium constant. The data represent the mean value from three independent experiments.

The concentration of 5-FU and BSA in the release medium was determined by WFZ-26A UV–visible spectrophotometer (Tianjin Science Instrument Plant, China). 5-FU content was calculated according to the absorption at 267 nm, and BSA content was calculated according to the absorption at 588 nm after being dyed with 1×10^{-4} g/mL Coomassie brilliant blue G250 solution. Before this analysis, the standard curves of 5-FU and BSA were calibrated. The accumulated release amount was calculated by Eq. (1):

$$E = \frac{V_E \sum_1^{n-1} C_i + V_0 C_n}{m_0} \times 100\% \quad (1)$$

where E is the accumulated release amount (%); V_E is the sampling volume (5 mL); V_0 is the initial volume, 10 mL; C_i and C_n are the drug concentrations (μg/mL); i and n are the sampling times; and m_0 is the mass of drug in gel (μg).

The DXM concentration in the release medium was determined by HPLC (Lab Alliance Model 201) with a Hypersil ODS-2 (250 mm × 4.6 mm) C18 column. The mobile phase composed of acetonitrile and water (62:38, v/v) was performed at a temperature of 30 °C and a flow rate of 1.0 mL/min. The peak of DXM was detected at 249 nm. Before this analysis, the standard curve of DXM was calibrated by HPLC. The accumulated release amount was also calculated according to Eq. (1).

2.7. Assay of in vitro cytotoxicity

Mouse embryonic fibroblast cells (3T3) were cultured on a 96-well tissue culture plates (100 μl/well; Cellstar) at 1×10^5 cells/mL in DMEM (Dullecco's modified Eagle's medium; Sigma–Aldrich, USA) containing 10% fetal bovine serum (FBS, Biochrom Ag, Germany), and then incubated at 37 °C in 5% CO_2 for 24 h. *N*-CS-g-mPEG-20 NP dispersion was sterilized by UV radiation for 1 h and then diluted with DMEM medium to obtain various solutions in the range of 40–200 μg/ml. 100 μl of each solution was separately added into the individual well to replace the original medium, in which 3T3 cells had been seeded. The cell viability cultured with DMEM medium was used as control. After incubation for 24 h, the cell viability was evaluated by MTT assay (Tang, Du, Hu, Shi, & Kennedy, 2007). The absorbance at 570 nm which represented the cell viability was measured with a Wellscan MK-3 Microplate Spectrophotometer (Labsystems Dragon, Finland) (Chung et al., 2005).

Statistical comparisons were performed by using one-way ANOVA with Origin software. P values less than 0.05 were considered statistically significant for all tests.

3. Results and discussion

3.1. Evaluation of N-CS-g-mPEG NPs

N-CS-g-mPEG can dissolve in deionized H_2O, and spontaneously form nanometer-sized aggregates by strong intermolecular hydrogen bonds between chitosan moieties (Deng, Qi, Yao, Feng, & Dong, 2007). The size morphology and distribution of *N*-CS-g-mPEG-20 aggregates in deionized H_2O are shown in Fig. 1. It can be seen from Fig. 1a that the *N*-CS-g-mPEG-20 NPs present spherical shape. As shown in Fig. 1b, the average diameter of *N*-CS-g-mPEG-20 NPs is less than 200 nm, and the size polydispersity index (PDI) is 0.182.

3.2. Thermoreversible hydrogel

The aqueous dispersions of *N*-CS-g-mPEG NP-FDP undergo reversible gel–sol transitions as the temperature changes. The phase transition diagrams of *N*-CS-g-mPEG NP aqueous dispersions were determined by a test tube inverting method. The aqueous dispersion (2 wt%) of *N*-CS-g-mPEG-20 NP-FDP (Fig. 2a) was prepared just by adding water into the bottle containing NP-FDP and slightly shaking at room temperature for 5 min. After being incubated at 4 °C for 12 h, the NP dispersion formed a non-flowing NP hydrogel (Fig. 2b). The hydrogel can transform to a free-flowing liquid (Fig. 2c) after heating to higher temperatures, and the liquid can become the non-flowing gel again as the temperature decreases. Furthermore, DS has a great influence transition temperature. For the same gel concentration, the transition temperature would decrease with the increment in DS. As shown in Fig. 2d, the hydrogel of *N*-CS-g-mPEG can be prepared with a wide range of temperature, including physiological temperature (37 °C).

3.3. Interior morphology of N-CS-g-mPEG NP hydrogel

The interior morphologies of *N*-CS-g-mPEG NP hydrogel observed by ESEM are shown in Fig. 3. The ESEM images clearly illustrate the dependence of the interior morphology of *N*-CS-g-mPEG NP hydrogel on DS. The *N*-CS-g-mPEG NP hydrogel exhibits a highly macroporous spongelike structure. For the same gel concentration, the porous structure becomes more compact and the pore size smaller with the increment in DS of *N*-CS-g-mPEG.

3.4. In vitro release behaviors

The *in vitro* release profiles of 5-FU, BSA and DXM from *N*-CS-g-mPEG NP hydrogels are shown in Fig. 4. The DS and gel concentration can influence the *in vitro* release rate of drug from *N*-CS-g-mPEG NP hydrogel. The cumulative releases of drugs are

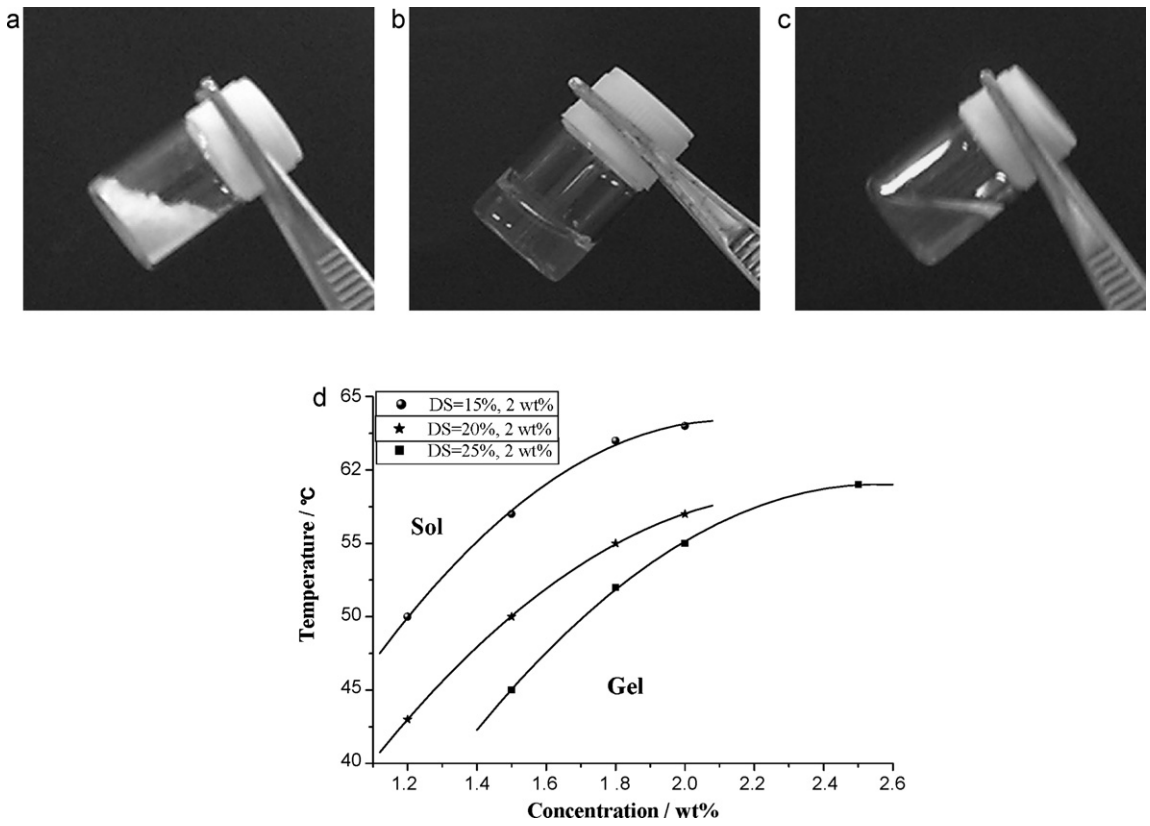

Fig. 2. Thermoreversible gel formation of *N*-CS-g-mPEG NP-FDP aqueous dispersion. (a) *N*-CS-g-mPEG-20 NP-FDP; (b) in situ gel of *N*-CS-g-mPEG-20 NP-FDP at 4 °C and body temperature; (c) aqueous dispersion of *N*-CS-g-mPEG-20 NP-FDP at 58 °C; (d) phase transition of aqueous dispersion of *N*-CS-g-mPEG NP-FDP.

decreased with increasing DS or gel concentration. For the same gel concentration, the cumulative releases of 5-FU (Fig. 4a), BSA (Fig. 4b) and DXM (Fig. 4c) are decreased with increasing DS. Simultaneously, for the same DS, the cumulative release of DXM (Fig. 4c) is decreased with increasing gel concentration. To the drug-loaded hydrogel, the drug can be released through different mechanisms (Molina, Li, Martinez, & Vert, 2001). The drug release can be driven by not only diffusion of drug but also erosion of the gel. However, the degradation of *N*-CS-g-mPEG NP hydrogels is so slow that the impact of degradation on the release can be ignored. Therefore, for the same drug, the gel network structure is the main factor of drug diffusion rate. Owing to the increment of DS and gel concentration, the network grid of hydrogels become smaller, which depress the diffusion rate of drug.

Comparing Fig. 4a with Fig. 4b, we found that the *in vitro* release rate of 5-FU is faster than that of BSA using the same *N*-CS-g-mPEG NP hydrogel as the carrier material. The initial burst releases of 5-FU from the drug-loaded *N*-CS-g-mPEG NP hydrogel are obviously observed and cumulative release reaches to 100% after 28 h. For BSA, the initial burst releases are not observed and sustained releases were achieved for more than 17 days. Due to the identity of employed hydrogel systems, the diffusion rate of drug was influenced by the properties of drug, including hydrophilicity and molecular weight. In general, the strong hydrophilicity and low molecular weight can make the drug diffusion fast. Although the hydrophilicity of 5-FU is similar to BSA, the molecular weight of BSA is approximate 637 times than that of 5-FU (M_n = 103.1). Therefore, the release rate of BSA is slower than that of 5-FU.

Comparing Fig. 4b with Fig. 4c, we found that the release rate of BSA is faster than that of DXM using the same *N*-CS-g-mPEG NP hydrogel. For example, although the molecular weight of BSA is approximate 167 times than that of DXM (M_n = 392.5), the hydrophilicity of BSA is much stronger than that of DXM. Moreover, BSA was loaded in the hydrophilic region while DXM was in the hydrophobic region of NP hydrogel. Therefore, BSA was directly released from hydrogels through drug diffusion. However, DXM must undergo the diffusion process from the hydrophobic to hydrophilic region, and then from the hydrophilic region of NP

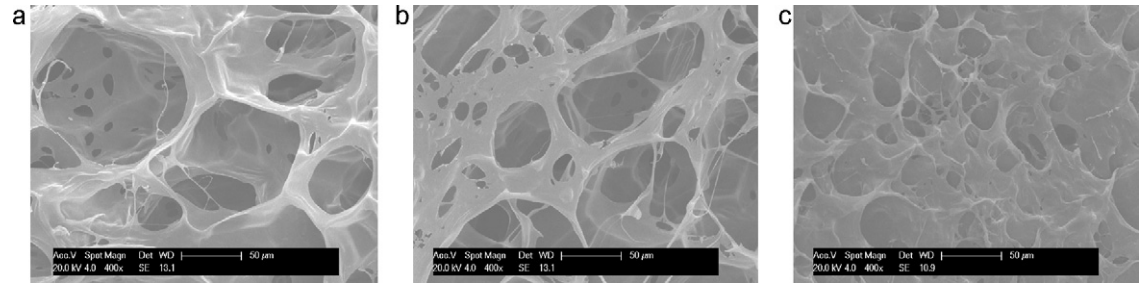

Fig. 3. ESEM photographs of *N*-CS-g-mPEG NP hydrogel (1000×). The concentration of polymer in hydrogel is 2 wt%. (a) *N*-CS-g-mPEG-15; (b) *N*-CS-g-mPEG-20; (c) *N*-CS-g-mPEG-25.

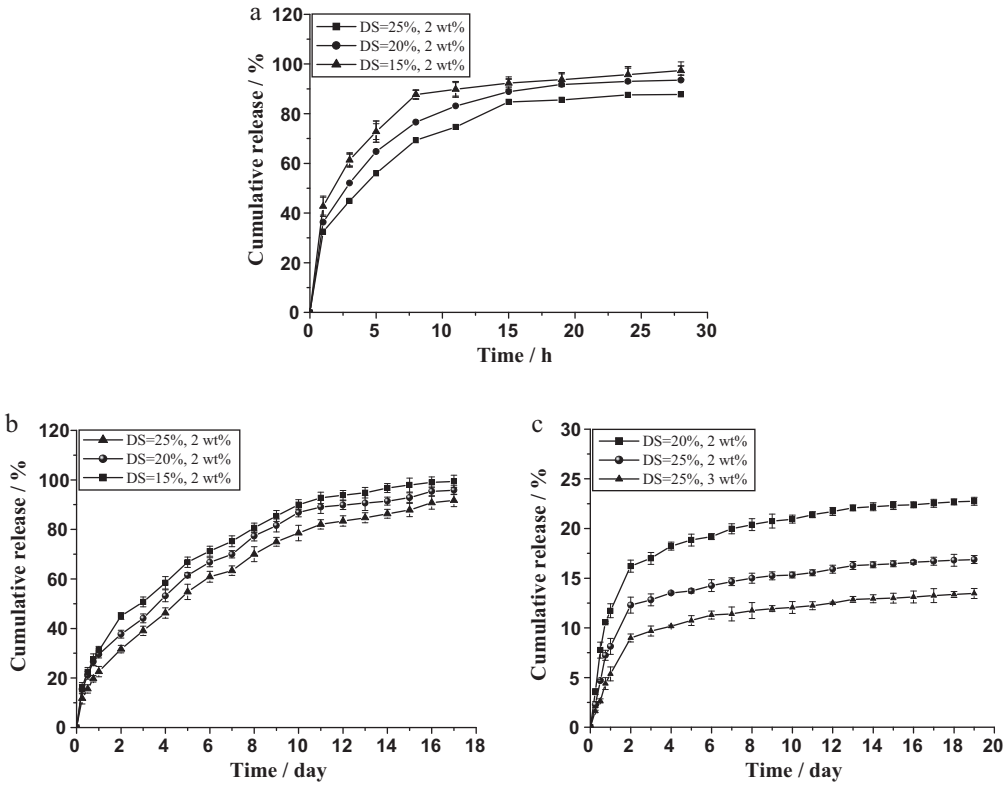

Fig. 4. *In vitro* release profile of 5-FU (a), BSA (b) and DXM (c) from *N*-CS-g-mPEG NP hydrogel at 37 °C. The concentration of polymer in hydrogel was 2–3 wt%, and the DS of *N*-CS-g-mPEG was 15%, 20% and 25%, respectively. PBS (pH 7.4) was used as the acceptor. The 5-FU-loaded, BSA-loaded and dexamethasone-loaded amounts are all 1 wt%. The data represent the mean value from three independent experiments.

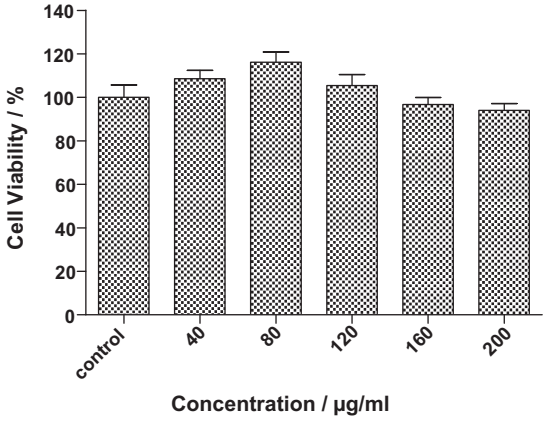

Fig. 5. *In vitro* cytotoxicity evaluation of *N*-CS-g-mPEG-20 ($n = 5$) (ANOVA, $P \leq 0.05$).

hydrogel to acceptor medium. Therefore, the *in vitro* release rate of DXM is slower than that of BSA.

To sum up, *N*-CS-g-mPEG NP hydrogel can provide a good controlled release for BSA and DXM.

3.5. *In vitro* cytotoxicity

The potential applications in the biomedical fields were assessed by investigating the cytotoxicity of *N*-CS-g-mPEG-20 NPs using the MTT assay. Mouse embryonic fibroblast cells (3T3) were used as model cell and the experimental groups without *N*-CS-g-mPEG-20 NPs was used as the control groups. The viability of 3T3 is illustrated in Fig. 5. Clearly, *N*-CS-g-mPEG-20 NPs show no or low cytotoxicity, as the cell viability cultured with DMEM medium containing *N*-CS-g-mPEG-20 (40–200 μg/mL) are at a similar level to that of control group. The relative viability of the cells is greater than 94%, according to the relationship of relative growth rate and cytotoxicity grade in United States Pharmacopeia (USP), indicating no apparent cytotoxicity of these materials towards the 3T3 cells.

4. Conclusions

In this paper, a thermoreversible hydrogels of *N*-CS-g-mPEG NPs were prepared, and their aqueous dispersion can undergo reversible gel–sol transition as the temperature changes. The size of *N*-CS-g-mPEG NPs with spherical shape is lower than 200 nm. The interior morphologies of *N*-CS-g-mPEG NP hydrogels exhibit a highly macroporous spongelike structure. Furthermore, *in vitro* drug release behaviors indicate that *N*-CS-g-mPEG NP hydrogel can provide a sustained release for BSA and DXM. The low toxicity towards 3T3 cells makes the *N*-CS-g-mPEG NP hydrogels be potential candidate carrier materials for the drug controlled delivery systems of hydrophobic and bio-macromolecular drugs.

Acknowledgements

This work had been supported by a grant from 863 Program (2009AA03Z313), National Grand Program on Key Infectious Disease Control (2008ZX10001-015-10), Tianjin Municipal Natural Science Foundation Key Project (08JCZDJC17200), and Tianjin Municipal Natural Science Foundation (08JCYBJC01800).

Appendix A. Supplementary data

Supplementary data associated with this article can be found, in the online version, at doi:10.1016/j.carbpol.2010.10.048.

References

Bhattarai, N., Gunn, J., & Zhang, M. (2010). Chitosan-based hydrogels for controlled, localized drug delivery. *Advanced Drug Delivery Reviews*, *62*, 83–99.

Bhattarai, N., Matsen, F. A., & Zhang, M. (2005). PEG-grafted chitosan as an injectable thermoreversible hydrogel. *Macromolecular Bioscience*, *5*, 107–111.

Bhattarai, N., Ramay, H. R., Gunn, J., Matsen, F. A., & Zhang, M. (2005). PEG-grafted chitosan as an injectable thermosensitive hydrogel for sustained protein release. *Journal of Controlled Release*, *103*, 609–624.

Chenite, A., Chaput, C., Wang, D., Combes, C., Buschmann, M. D., Hoemann, C. D., et al. (2000). Novel injectable neutral solutions of chitosan form biodegradable gels in situ. *Biomaterials*, *21*, 2155–2161.

Chung, H. J., Go, D. H., Bae, J. W., Jung, I. K., Lee, J. W., & Park, K. D. (2005). Synthesis and characterization of Pluronic-grafted chitosan copolymer as a novel injectable biomaterial. *Current Applied Physics*, *5*, 485–488.

Coughlan, D. C., Quilty, F. P., & Corrigan, O. I. (2004). Effect of drug physicochemical properties on swelling/deswelling kinetics and pulsatile drug release from thermoresponsive poly(N-isopropylacrylamide) hydrogels. *Journal of Controlled Release*, *98*, 97–114.

Deng, L. D., Qi, H. Y., Yao, C. M., Feng, M. H., & Dong, A. J. (2007). Investigation on the properties of methoxy poly(ethylene glycol)/chitosan graft co-polymers. *Journal of Biomaterials Science-Polymer Edition*, *18*, 1575–1589.

Denkbas, E. B., & Ottenbrite, R. M. (2006). Perspectives on: Chitosan drug delivery systems based on their geometries. *Journal of Bioactive and Compatible Polymers*, *21*, 351–368.

DesNoyer, J. R., & McHugh, A. J. (2003). The effect of Pluronic on the protein release kinetics of an injectable drug delivery system. *Journal of Controlled Release*, *86*, 15–24.

Exner, A. A., Krupka, T. M., Scherrer, K., & Teets, J. M. (2005). Enhancement of carboplatin toxicity by Pluronic block copolymers. *Journal of Controlled Release*, *106*, 188–197.

Gong, C. Y., Qian, Z. Y., Liu, C. B., Huang, M. J., Gu, Y. C., Wen, Y. J., et al. (2007). A thermosensitive hydrogel based on biodegradable amphiphilic poly(ethylene glycol)–polycaprolactone–poly(ethylene glycol) block copolymers. *Smart Materials and Structures*, *16*, 927–933.

Hatefi, A., & Amsden, B. (2002). Biodegradable injectable in situ forming drug delivery systems. *Journal of Controlled Release*, *80*, 9–28.

Hoffnam, A. S. (2002). Hydrogels for biomedical applications. *Advanced Drug Delivery Review*, *54*, 3–12.

Jeon, O., Lee, S. H., Kim, S. H., Lee, Y. M., & Kim, Y. H. (2003). Synthesis and characterization of poly(L-lactide)–poly(ε-caprolactone) multiblock copolymers. *Macromolecules*, *36*, 5585–5592.

Jeong, B., Kim, S. W., & Bae, Y. H. (2002). Thermosensitive sol–gel reversible hydrogels. *Advanced Drug Delivery Review*, *54*, 37–51.

Jeong, Y. I., Kim, D. G., Jang, M. K., & Nah, J. W. (2008). Preparation and spectroscopic characterization of methoxy poly(ethylene glycol)-grafted water-soluble chitosan. *Carbohydrate Research*, *343*, 282–289.

Jin, R., Moreira Teixeira, L. S., Dijkstra, P. J., Karperien, M., van Blitterswijk, C. A., Zhong, Z. Y., et al. (2009). Injectable chitosan-based hydrogels for cartilage tissue engineering. *Biomaterials*, *30*, 2544–2551.

Joo, M. K., Park, M. H., Choi, B. G., & Jeong, B. (2009). Reverse thermogelling biodegradable polymer aqueous solutions. *Journal of Materials Chemistry*, *19*, 5891–5905.

Kumar, M. N., Muzzarelli, R. A., Muzzarelli, C., Sashiwa, H., & Domb, A. J. (2004). Chitosan chemistry and pharmaceutical perspectives. *Chemical Reviews*, *104*, 6017–6084.

Lehr, C. M., Bouwstra, J. A., Schacht, E. H., & Junginger, H. E. (1992). In vitro evaluation of mucoadhesive properties of chitosan and some other natural polymers. *International Journal of Pharmaceutics*, *78*, 43–48.

Lin, X. N., Zhou, R. M., Qiao, Y., Jin, F. M., Zhai, Y. L., Xing, J. F., et al. (2008). Poly(ethylene glycol)/poly(ethyl cyanoacrylate) amphiphilic triblock copolymer nanoparticles as delivery vehicles for dexamethasone. *Journal of Polymer Science Part A: Polymer Chemistry*, *46*, 7809–7815.

Maeda, Y., & Yamabe, M. (2009). A unique phase behavior of random copolymer of *N*-isopropylacrylamide and *N*,*N*-diethylacrylamide in water. *Polymer*, *50*, 519–523.

Mi, F. L., Shyu, S. S., Chen, C. T., & Schoung, J. Y. (1999). Porous chitosan microsphere for controlling the antigen release of Newcastle disease vaccine: Preparation of antigen-adsorbed microsphere and in vitro release. *Biomaterials*, *20*, 1603–1612.

Molina, I., Li, S., Martinez, M. B., & Vert, M. (2001). Protein release from physically crosslinked hydrogels of the PLA/PEO/PLA triblock copolymer-type. *Biomaterials*, *22*, 363–369.

Muzzarelli, R. A. A. (1997). Human enzymatic activities related to the therapeutic administration of chitin derivatives. *Cellular and Molecular Life Sciences*, *53*, 131–140.

Park, K., Kim, J. H., Nam, Y. S., Lee, S., Nam, H. Y., Kim, K., et al. (2007). Effect of polymer molecular weight on the tumor targeting characteristics of self-assembled glycol chitosan nanoparticles. *Journal of Controlled Release*, *122*, 305–314.

Park, K. M., Lee, S. Y., Joung, Y. K., Na, J. S., Lee, M. C., & Park, K. D. (2009). Thermosensitive chitosan–Pluronic hydrogel as an injectable cell delivery carrier for cartilage regeneration. *Acta Biomaterialia*, *5*, 1956–1965.

Qiu, Y., & Park, K. (2001). Environment-sensitive hydrogels for drug delivery. *Advanced Drug Delivery Review*, *53*, 321–339.

Roques, C., Salmon, A., Fiszman, M. Y., Fattal, E., & Fromes, Y. (2007). Intrapericardial administration of novel DNA formulations based on thermosensitive Poloxamer 407 gel. *International Journal of Pharmaceutics*, *331*, 220–223.

Roughley, P., Hoemann, C., DesRosiers, E., Mwale, F., Antoniou, J., & Alini, M. (2006). The potential of chitosan-based gels containing intervertebral disc cells for nucleus pulposus supplementation. *Biomaterials*, *27*, 388–396.

Shim, W. S., Kim, J.-H., Park, H., Kim, K., Kwon, I. C., & Lee, D. S. (2006). Biodegradability and biocompatibility of a pH- and thermo-sensitive hydrogel formed from a sulfonamide-modified poly(ε-caprolactone-*co*-lactide)–poly(ethylene glycol)–poly(ε-caprolactone-*co*-lactide) block copolymer. *Biomaterials*, *27*, 5178–5185.

Shu, X. Z., Liu, Y. C., Palumbo, F. S., Luo, Y., & Prestwich, G. D. (2004). In situ crosslinkable hyaluronan hydrogels for tissue engineering. *Biomaterials*, *25*, 1339–1348.

Sombatmankhong, K., Sanchavanakit, N., Pavasant, P., & Supaphol, P. (2007). Bone scaffolds from electrospun fiber mats of poly(3-hydroxybutyrate), poly(3-hydroxybutyrate-*co*-3-hydroxyvalerate) and their blend. *Polymer*, *48*, 1419–1427.

Tang, Y. F., Du, Y. M., Hu, X. W., Shi, X. W., & Kennedy, J. F. (2007). Rheological characterisation of a novel thermosensitive chitosan poly(vinyl alcohol) blend hydrogel. *Carbohydrate Polymers*, *67*, 491–499.

Temenoff, J. S., & Mikos, A. G. (2000). Injectable biodegradable materials for orthopedic tissue engineering. *Biomaterials*, *21*, 2405–2412.

van der Merwe, S. M., Verhoef, J. C., Verheijden, J. H. M., Kotzé, A. F., & Junginger, H. E. (2004). Trimethylated chitosan as polymeric absorption enhancer for improved peroral delivery of peptide drugs. *European Journal of Pharmaceutics and Biopharmaceutics*, *58*, 225–235.

Wu, J., Su, Z. G., & Ma, G. H. (2006). A thermo- and pH-sensitive hydrogel composed of quaternized chitosan/glycerophosphate. *International Journal of Pharmaceutics*, *315*, 1–11.

Zhai, Y. L., Qiao, Y., Xie, C. P., Lin, X. N., Ma, Y. Z., Dong, A. J., et al. (2008). Preparation and *in vitro* release of D,L-tetrahydropalmatine-loaded graft copolymer nanoparticles. *Journal of Applied Polymer Science*, *110*, 3525–3531.

Zhang, J. T., Bhat, R., & Jandt, K. D. (2009). Temperature-sensitive PVA/PNIPAAm semi-IPN hydrogels with enhanced responsive properties. *Acta Biomaterialia*, *5*, 488–497.